Grazing-incidence x-ray diffraction study of Langmuir films of amphiphilic monodendrons

Wen-Jung Pao, Fan Zhang, and Paul A. Heiney*

Department of Physics and Astronomy, and Laboratory for Research on the Structure of Matter,
University of Pennsylvania, Philadelphia, Pennsylvania 19104

Catherine Mitchell,[†] Wook-Dong Cho,[‡] and Virgil Percec

Roy and Diana Vagelos Laboratories, Department of Chemistry and Laboratory for Research on the Structure of Matter,
University of Pennsylvania, Philadelphia, Pennsylvania 19104

We have used pressure-area isotherms and grazing-incidence x-ray diffraction to study structures of Langmuir films of first-generation monodendrons with two or three peripheral alkyl chains. Unlike the structures observed in their bulk liquid crystalline mesophases, these multichain monodendrons form either a centered rectangular lattice with molecular axes tilted toward nearest neighbors or an oblique lattice with molecular axes tilted in low-symmetry directions.

I. INTRODUCTION

Langmuir films, composed of amphiphilic molecules adsorbed at the air-water interface, continue to attract widespread attention due to their importance as models for two-dimensional structures and phase transitions, as model biological membranes, and as precursors for technologically important Langmuir-Blodgett films [1–4]. In recent years, the field has advanced greatly due to the development of synchrotron x-ray scattering and surface microscopy techniques [5–7].

The vast majority of films studied have been composed of linear molecules with a hydrophilic end group and a hydrophobic alkyl tail. Such molecules generally form a close-packed structure in the compressed state, possibly with some tilt of the molecular axes. Less attention has been paid to other molecular geometries. A crown ether modified with two alkyl chains appeared to form a close-packed structure with variable chain tilt [8]. Phospholipid molecules with two hydrophobic chains have been heavily studied due to their importance in biological membranes [9,10]. Langmuir films composed of disk-shaped molecules (such as those that are responsible for the formation of discotic liquid crystals) typically pack in an "edge-on" arrangement, with columns of molecules running parallel to the water surface [11–14]. In most of these cases only one peak is observed in grazing-incidence diffraction measurements, which limits the amount of structural information that can be inferred.

Molecular and supramolecular monodendrons form a powerful route to forming crystalline and liquid-crystalline structures with precisely controlled structure and functionality [15–18]. The monodendron shape is determined by the

molecular architecture of the repeat unit, the generation number, and the functionality both on the periphery and in the apex. Depending on the width of the aliphatic (peripheral) end and the apex (core), the monodendrons might be described as tapers, half disk, disks, pyramids, cones, half spheres, or spheres, resulting in lamellar, columnar, or cubic macroscopic lattices [19]. Although the bulk structures and phases of dendrimers have been heavily studied, less is known about their behavior at solid or liquid interfaces [20–24]. We recently used x-ray reflectivity to study a series of second and third-generation monodendrons with hydrophobic $C_{12}H_{25}$ alkyl tails at the periphery and hydrophilic COOH, CO_2CH_3, or crown ether groups in the core [24]. We found that they were best described by a model in which the hydrophilic core was at or beneath the water surface, there was a low-density region just above the surface, and the alkyl chains formed a high-density sublayer above the surface with the chains directed perpendicular to the interface. In the present paper we extend this program with a grazing-incidence diffraction study of closely related monomers with two and three alkyl chains.

We used pressure-area (Π-A) isotherms and grazing incidence x-ray diffraction (GID) to study first-generation monodendrons **1** and **2** with two and three hydrocarbon [1] chains at the periphery, respectively (Fig. 1). The peripheral hydrophobic alkyl chains are $C_{12}H_{25}$, the hydrophilic polar groups are formed by CH_2OH in the cores, and these two parts are connected by rigid aromatic benzene rings that form the branching backbones for these multichain molecules.

We found only one distinct compressed phase for both compounds from the isotherm measurements. GID studies in the compressed state showed well-resolved diffraction peaks for compound 1 not seen in similar two-chain molecular films [6,9,25–27].

II. EXPERIMENTAL METHODS

Compounds **1** and **2** were synthesized as described elsewhere [28]. Small amounts ($\sim 10^{-3}$ g) were weighed on a

---

*Author to whom correspondence should be addressed. Email address: heiney@physics.upenn.edu

[†]Present address: Cognis Deutschland GmbH & Co. KG, Henkelstrasse 67, D-40551 Düsseldorf, Germany.

[‡]Present address: The Scripps Research Institute, 10550 North Torrey Pines Road, La Jolla, CA 92037.
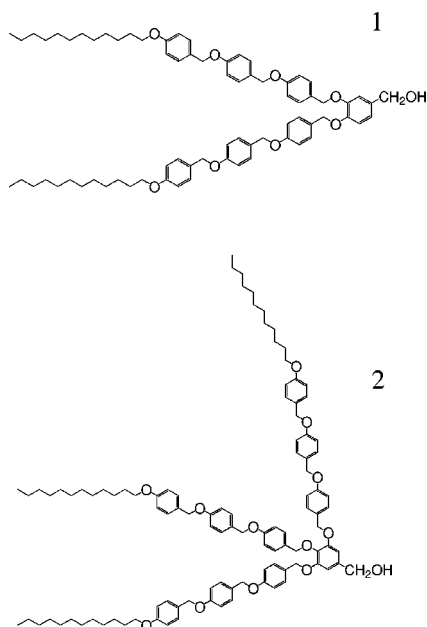
FIG. 1. 1: A first-generation monodendron with two hydrocarbon chains (top). 2: A first-generation monodendron with three hydrocarbon chains (bottom).

FIG. 2. Pressure-area isotherms of monolayers of dendritic compounds **1** and **2**.

Denver Instrument AD-200DS electronic balance to an accuracy of 10^{-5} g. The solute was then dissolved in high performance liquid chromatography grade chloroform (99.9% pure) to make dilute solutions of concentration ranging from 10^{-3} M to 10^{-4} M. The subphase water was purified using a Millipore filtration system with a resistivity $\rho > 18.2$ MΩ cm. We typically deposited 50–100 μl of solution on the water surface for isotherm or GID measurements.

The Langmuir trough employed for the *in situ* has dimensions of 160×476 mm^2 and a compression ratio of more than 9.0. Π-A isotherms were collected both at the University of Pennsylvania, using a Lauda film balance, and *in situ* during the x-ray measurements, using a Wilhelmy plate [1]. The Lauda balance and Wilhelmy plate were adjusted for zero surface tension with a pure water subphase; the Lauda balance was calibrated using a standard weight and the Wilhelmy plate was calibrated using the difference of surface tensions of pure water subphase and air. The two measurements gave consistent results, but the Wilhelmy plate was found to be less suitable at higher surface pressures. The films were sufficiently stiff that the plate was sometimes tilted sideways or even pushed out of the film. Therefore, during the course of the x-ray measurements we relied primarily on molecular surface areas to establish a connection with previously determined Π-A isotherms.

During the diffraction measurements, the subphase water temperature was maintained at 15 °C. The films were compressed to a surface pressure in the range of 15–20 mN/m, and measurements were then made at fixed area. The Langmuir trough was located in a sealed chamber, which was flushed with humidified He to lower background air scattering and minimize evaporation.

GID measurements were conducted using the liquid surface spectrometer at beam line 9ID, CMC-CAT, of the Advanced Photon Source (APS), Argonne National Laboratory. The x-ray optics were similar to those described elsewhere [11–13,29]. A Ge (111) crystal deflected a monochromatic beam of wavelength $\lambda = 1.240$ Å toward the film surface at an angle slightly smaller than the critical angle for total reflection. Söller slits between the sample and detector provided additional collimation in the scattering plane. A linear position sensitive detector (PSD) was mounted on the 2θ arm so that scattered intensity was measured as a function of both the in-plane momentum transfer Q_{xy} and the out-of-plane momentum transfer Q_z. We define the in-plane momentum transfer to be $Q_{xy} = 4\pi \sin(\theta)/\lambda$, where 2θ is the scattering angle in the horizontal plane. This approximation neglects small corrections arising from the out-of-plane component of the momentum transfer.
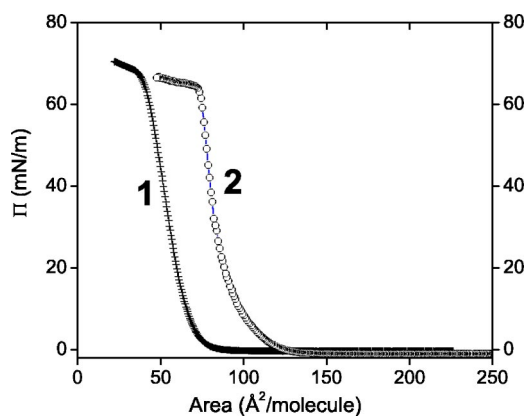
The resulting instrumental resolution in the scattering plane was $\Delta Q_{xy} = 0.002$ Å^{-1} full width at half maximum (FWHM). At each setting of Q_{xy}, the PSD collected photons in the range -0.15 Å$^{-1} \leq Q_z \leq 0.91$ Å^{-1}. We will refer to the sum of all counts in the PSD at a particular Q_{xy} as the "Q_z-integrated intensity." Since our films are believed to have no preferred orientation, these intensities correspond to a two-dimensional powder diffraction pattern. The resolution in Q_z was 0.004 Å^{-1} FWHM. GID scans were performed in the range $1° \leq 2\theta \leq 25°$ (0.09 Å$^{-1} \leq Q_{xy} \leq 2.19$ Å^{-1}). In general we observed strong powder diffraction peaks near $2\theta \approx 15°$–$22°$ ($Q_{xy} \approx 1.3$–2.0 Å^{-1}).

Our samples were somewhat sensitive to radiation damage. After 30 min or more in the primary beam, the exposed part of the film was damaged, as demonstrated by decreasing diffraction peak intensities. We minimized radiation damage by keeping the x-ray shutters closed as much as possible and by frequently translating the sample in the beam. We performed cross-checks to verify that peak positions and profiles were not highly sensitive to radiation damage over the 10-20 minute time scale of a typical exposure.

III. RESULTS AND DISCUSSION

The Π-A isotherms (Fig. 2) for compounds **1** and **2** showed only one stable compressed solid phase above the dilute gas phase.
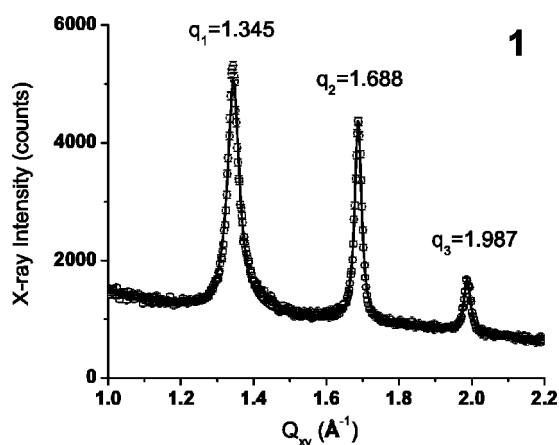
FIG. 3. GID patterns from a monolayer of two-chain molecules **1** compressed to 44 Å^2/molecule. Points show measured Q_z-integrated intensity as a function of in-plane momentum transfer; the solid line is a fit to the Lorentzian line shape.

FIG. 4. Contour plot of the intensity distribution in the Q_{xy}-Q_z plane for compound **1**.

When the films were further compressed to above 65 mN/m, they became unstable to multilayer formation. This critical pressure is slightly larger than that of arachidic acid films (55 mN/m) measured with the same Lauda film balance, and reflects the high stability of these films both to multilayer formation and subphase dissolution. The molecular area for compound **1** (two chains) varies between 68 Å^2/molecule and 45 Å^2/molecule in the compressed phase; the corresponding values for compound **2** (three chains) are 90 Å^2/molecule and 75 Å^2/molecule. (These values were calculated by extrapolating the linear steep portions of the isotherms to zero pressure and to the point of inflection at high pressure.) Thus, the area per chain ranges between 23 and 34 Å^2 for compound **1** and between 25 and 30 Å^2 for compound **2**. These results are easily explained if the tails are somewhat ''splayed'' or tilted out at the onset of the riser, and close packed at full compression. The maximally compressed areas are comparable to those of compressed Langmuir films formed by rodlike, single alkyl chain amphiphiles [30]. For example, the limiting areas for monolayers of arachidic acid are 24 Å^2/molecule for the tilted compressed phase and 20 Å^2/molecule in the nontilt, higher-pressure compressed phase. GID measurements on compound **1** were made at a fixed molecular area of 44 ±2 Å^2/molecule, and those on compound **2** were made at a fixed molecular area of 60±2 Å^2/molecule.

The Q_z-integrated intensity for compound **1** is shown in Fig. 3. The d spacings of the strong peaks are all in the range of 3–5 Å, comparable to typical distances between neighboring parallel chains. This clearly demonstrates that the in-plane structure is essentially lamellar, and is dominated by close packing of the alkyl chains. Such a structure is in marked contrast to the bulk liquid-crystalline mesophases of monodendrons, which show much larger lattice parameters determined by the end-to-end length of the molecules [16–18]. The sharpness of the peaks indicates the existence of long range (or quasi-long-range) in-plane structural order. Peak positions and widths were obtained from least-squares fits of the first three peaks to a Lorentzian line shape. The
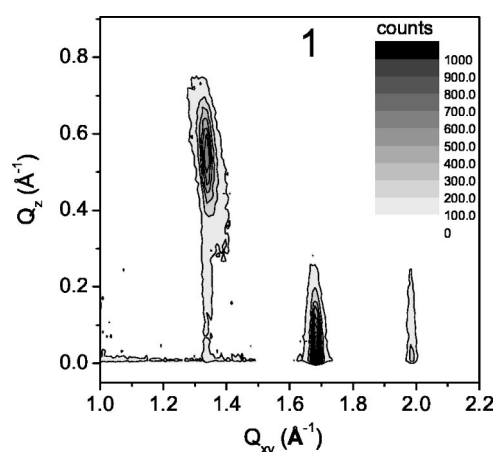
peak positions of compound **1** were well indexed as the (1,1), (2,0), and (0,2) reflections of a centered rectangular lattice with lattice parameters $a = 7.44$ Å, $b = 6.32$ Å. (This structure can alternatively be thought of as a slight distortion of a hexagonal lattice to give an oblique lattice with lattice parameters $a' = b' = 4.88$ Å and an angle of 99.3°, rather than 120°, between them.) The FWHM for the first three peaks in Fig. 3 are 0.040 Å^{-1}, 0.023 Å^{-1}, and 0.022 Å^{-1}, respectively. The corresponding correlation lengths are 160 Å, 270 Å, and 280 Å for the three peaks of the in-plane lattice of compound **1**.

From the lattice parameters a, b, we can calculate the area of the unit cell of the in-plane centered rectangular lattice. For compound **1**, the calculated area is 47.0 Å^2. We note that this is equal within experimental uncertainty to the molecular area at the surface concentration chosen. A hexagonal or centered rectangular lattice would be the normal result of close packing of identical alkyl chains. Alternate structures can be considered. A herringbone or other simple rectangular structure would result in finite intensity for mixed odd-even index rectangular peaks such as the (2,1). Since such peaks are not observed, the scattering must be dominated by the peripheral alkyl chains, which occupy equivalent positions in the centered rectangular lattice. The apical benzene rings do, however, play a role. They result in a lattice that is somewhat dilated compared to that expected for bare alkyl chains, they slightly modify the Q_z dependence of the observed peaks, and they prevent the formation of rotator phases [31] seen in monolayers of single-rod amphiphiles [32,33].

Figure 4 shows that the diffracted intensity forms rods in the Q_{xy}-Q_z plane, and that for some of the peaks the maximum is at finite Q_z. To analyze these results, we model the chains as rods of charge, possibly tilted away from the normal. The extent of the Bragg rods depends inversely on the length L' of the molecular rod, and the effect of tilting the rod is to move the diffraction maximum to finite Q_z. We take L' to be the true length of the rod and $L = L' \cos \tau$ to be the projection of the rod length on the z axis normal to the interface, with τ being the tilt angle. We then calculate the square of the molecular form factor to be
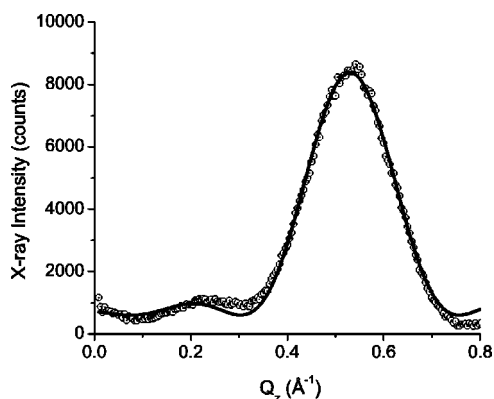
FIG. 5. A Bragg rod scan as a function of Q_z for sample **1** measured at $Q_{xy} = 1.345$ Å^{-1}.

$$I(Q_z) = I_0 \left[\frac{\sin\left((Q_z - Q_z^{peak}) \frac{L}{2} \right)}{(Q_z - Q_z^{peak}) \frac{L}{2}} \right]^2 \qquad (1)$$

Figure 5 shows a fit to the Q_z dependence of the intensity of compound **1** at $Q_{xy} = 1.345$ Å^{-1} to the functional form in Eq. (1). The best fit gives $Q_z^{peak} = 0.530$ Å^{-1} and $L = 27.94$ Å.

We can now calculate [29,34,35] the tilt angle τ from the fitted value of Q_z^{peak}. For a particular peak with Bragg indices $(h,k,0)$, the tilt angle and peak position are related by

$$\tan(\tau) \sin(\Psi_{hk}) = \frac{Q_z^{peak}}{Q_{xy}}, \qquad (2)$$

where τ is the tilt angle of the rods away from the z axis, Ψ_{hk} is the azimuthal angle defined by the the projection of the tilt and the diffraction planes (i.e., zero if the tilt projection is parallel to or along the diffraction planes), Q_z^{peak} is the position of the intensity maximum along the Q_z axis, and Q_{xy} is the horizontal component of the momentum transfer that meets the Bragg law. In the case of compound 1, the rods tilt toward nearest neighbors, and therefore the tilt projection is along the $(1,1)$ direction in the hexagonal basis vectors. From the fit in Fig. 5 we calculate a tilt angle of $\tau \simeq 27.3°$. This implies that the molecular rod length is $L' = L/\cos(\tau) \approx 31.44 \pm 0.10$ Å.

The standard estimate [34] of the length ℓ of a fully extended $(CH_2)_n CH_3$ alkyl chain, assumed to be in the *all-trans* configuration, is $\ell_{n+1} = (n + \frac{9}{8}) 1.265$ Å, which in our case gives $\ell_{12} = 15.3$ Å. This is consistent with simple molecular modeling using Chem3D^{TM}, which provides an estimated length of the core benzene-ring portion of the molecule at 17.0 Å. Thus, the length of fully extended branches (i.e., alkyl chain plus three branched benzene rings) is approximately 33 Å. A comparison of the first two peaks indicates that the tilt angle of the chain should be towards a nearest-neighbor chain. This model, however, requires some fine tuning to explain the profile of the third peak. If the scattering were completely determined by the alkyl chains,
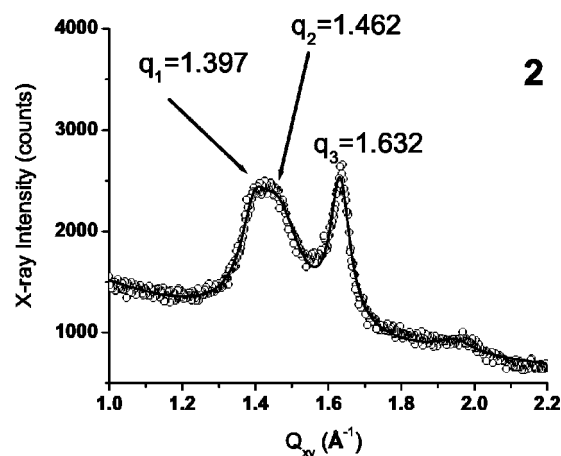
FIG. 6. GID patterns from a monolayer of three-chain molecules **2** at fixed area of 60 Å^2/molecule. Points show measured Q_z-integrated intensity as a function of in-plane momentum transfer; the solid line is a fit to the Lorentzian line shape.

we should observe a peak at $Q_z = 1.03$ Å^{-1}, outside the range of our measurements. The intensity and Q_z dependence of the third peak in Fig. 3 arises from the much weaker contribution of lower density, and nontilted, aromatic portion of the molecule that is close to the water surface. This is consistent with our earlier reflectivity measurements [24] of similar monodendrons, which indicated a lower electron density of the aromatic apical region than the aliphatic tails. Thus, a model that is quantitatively consistent with all the data has the benzene rings close the water surface contributing weakly to all three peaks, and tilted chains well above the subphase dominating the intensities of the first two peaks.

With the assumption that the chains are uniformly tilted in one direction, we can calculate the area of the unit cell projected in the plane normal to the molecular axes, i.e., $A_0 = A \cos(\tau) \approx 47 \cos(27.3°)$ Å$^2 = 42$ Å^2, corresponding to a chain area of 21.0 Å^2, only 5% larger than literature values for amphiphiles such as arachidic acid [30,35].

Note that the centered rectangular phase observed in compound **1** is a consequence, not just of the molecular tilt (which serves to break the hexagonal symmetry) but also of the noncircular cross section of the molecule and the fact that the chains are bonded to the apical benzene region, which constrains their possible motions. Even if the tilt angle were reduced by further compression, we would not expect to obtain a hexagonal lattice, unlike simpler amphiphiles with a rotator II phase [31,36].

Figures 6 and 7 show the Q_z-integrated intensity and intensity distribution, respectively, of the three-chain compound **2**. Fits to the GID pattern in Fig. 6 for molecule **2** yield peaks at $Q_{xy} = 1.397$ Å^{-1}, 1.462 Å^{-1}, and 1.632 Å^{-1}, with peak widths 0.086 Å^{-1}, 0.15 Å^{-1}, and 0.066 Å^{-1}, and corresponding correlation lengths of 73 Å, 41 Å, and 96 Å. These can be indexed as the $(1,0)$, $(0,1)$, and $(1,\bar{1})$ diffraction peaks of an oblique lattice with $a = 4.80$ Å, $b = 4.95$ Å, and included angle 110.4°. From these parameters we calculate [31] a unit-cell area of 22.27 Å^2, approximately equal to the area of a single alkyl chain. The tilt direction can be inferred
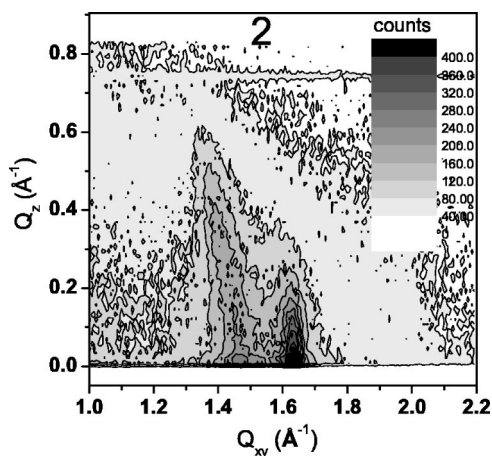
FIG. 7. Contour plot of the intensity distribution in the Q_{xy}-Q_z plane for compound **2**.

from the splitting of the first three peaks. In the case of close-packed hexagonal lattices with no tilt, the first diffraction peak is a degenerate multiplet consisting of the $(1,0)$, $(0,1)$, and $(1,\bar{1})$ Bragg peaks. For tilt along the nearest neighbor (NN) direction [i.e., $(1,1)$], the first peak from $(1,0)$ and $(0,1)$ is split from the second peak from $(1,\bar{1})$, as well as the case for tilt along the next nearest neighbor (NNN) direction. However, in the case of lower-symmetry tilt (i.e., neither NN nor NNN), the $(1,0)$, $(0,1)$, and $(1,\bar{1})$ peaks are all resolved.

From the analysis of a Bragg rod scan at Q_{xy} $=1.412$ Å^{-1} (i.e., neither at 1.397 Å^{-1} nor at 1.462 Å^{-1}, but between them and nearer to the first peak) we estimate the tilt angle in the range of $20°$–$24°$, along a lower-symmetry direction. With this estimated tilt angle, we find the area per chain in the plane normal to the molecular axis to be in the range 20.3–20.9 Å^2, which is 2–5% larger than the literature value.

The d spacings of the powder diffraction peaks indicate that the lateral features in the compressed phase arise primarily from ordered close packing of the peripheral alkyl chains. In the simpler two-chain molecular film, which showed extremely well-resolved peaks not seen in similar two-chain amphiphiles [6,9,25–27], the fully stretched alkyl chains formed a planar centered rectangular lattice with an uniform tilt of 27° towards their nearest neighbors.

One feature that distinguishes our compounds from more commonly studied amphiphiles is the noncircular cross section of the component molecules. Langmuir films of normal single-chain amphiphiles are often described as rotator phases [31] similar to those observed in bulk paraffin structures [36]. Such dynamic behavior is very unlikely in the present case, because of the large energy barriers to rotation of either the entire molecule or the individual alkyl chains relative to the rest of the molecule.

Tsukruk and co-workers [37,38] have recently used GID and x-ray reflectivity to study Langmuir films of low-generation monodendrons containing a crown-ether polar group, azobenzene spacer, and a varying number of peripheral alkyl chains. Their results are consistent with ours in showing a substantial chain tilt arising from the size mismatch between the apical and peripheral regions.

IV. SUMMARY

We have used GID to study the compressed solid phases of multichain monodendron Langmuir monolayers. We observe multiple, strong, well-resolved diffraction peaks indicating a high degree of structural order. We observe a centered rectangular lattice in compound 1 and an oblique lattice in compound 2, in both cases accompanied by molecular tilt. These results may serve as a starting point for further exploration into the structures and structure-function relations of Langmuir and solid films of more complex dendrimers.

[1] G.L. Gaines, *Insoluble Monolayers at Liquid-Gas Interfaces* (Interscience, New York, 1966).

[2] V.M. Kaganer, H. Möhwald, and P. Dutta, Rev. Mod. Phys. **71**, 779 (1999).

[3] R.M. Kenn, C. Bohm, A.M. Bibo, I.R. Peterson, H. Möhwald, J. Als-Nielsen, and K. Kjaer, J. Phys. Chem. **95**, 2092 (1991).

[4] D.B. Zhu, C. Yang, Y.Q. Liu, and Y. Xu, Thin Solid Films **210**, 205 (1992).

[5] P. Dutta, J.B. Peng, B. Lin, J.B. Ketterson, M. Prakash, P. Georgopoulos, and S. Ehrlich, Phys. Rev. Lett. **58**, 2228

(1987).

[6] K. Kjaer, J. Als-Nielsen, C.A. Helm, L.A. Laxhuber, and H. Möhwald, Phys. Rev. Lett. **58**, 2224 (1987).

[7] B. Berge, L. Faucheux, K. Schwab, and A. Libchaber, Nature (London) **350**, 322 (1991).

[8] P.A. Heiney, M.R. Stetzer, O.Y. Mindyuk, E. DiMasi, A.R. McGhie, H. Liu, and A.B. Smith, III, J. Phys. Chem. B **103**, 6206 (1999).

[9] C.A. Helm, H. Möhwald, K. Kjaer, and J. Als-Nielsen, Biophys. J. **52**, 381 (1987).

[10] K. Kjaer, J. Als-Nielsen, C.A. Helm, P. Tippmannkrayer, and H. Möhwald, Thin Solid Films **159**, 17 (1988).

[11] D. Gidalevitz, O.Y. Mindyuk, P.A. Heiney, B.M. Ocko, P. Henderson, H. Ringsdorf, N. Boden, R.J. Bushby, P.S. Martin, J. Strzalka, *et al.* J. Phys. Chem. B **101**, 10870 (1997).

[12] D. Gidalevitz, O.Y. Mindyuk, M.R. Stetzer, P.A. Heiney, M.L. Kurnaz, D.K. Schwartz, B.M. Ocko, J.P. McCauley, and A.B. Smith, III, J. Phys. Chem. B **102**, 6688 (1998).

[13] D. Gidalevitz, O.Y. Mindyuk, P.A. Heiney, B.M. Ocko, M.L. Kurnaz, and D.K. Schwartz, Langmuir **14**, 2910 (1998).

[14] O.Y. Mindyuk and P.A. Heiney, Adv. Mater. **11**, 341 (1999).

[15] V. Percec, P.W. Chu, G. Ungar, and J.P. Zhou, J. Am. Chem. Soc. **117**, 11441 (1995).

[16] S.D. Hudson, H.T. Jung, V. Percec, W.D. Cho, G. Johansson, G. Ungar, and V.S.K. Balagurusamy, Science **278**, 449 (1997).

[17] V.S.K. Balagurusamy, G. Ungar, V. Percec, and G. Johansson, J. Am. Chem. Soc. **119**, 1539 (1997).

[18] H. Duan, S. Hudson, G. Ungar, M.N. Holerca, and V. Percec, Chem. Eur. J. **7**, 4134 (2001).

[19] V. Percec, W.D. Cho, G. Ungar, and D.J.P. Yeardley, Angew. Chem. Int. Ed. Engl. **39**, 1598 (2000).

[20] V.V. Tsukruk, Adv. Mater. **10**, 253 (1998).

[21] P.M. Saville, J.W. White, C.J. Hawker, K.L. Wooley, and J.M.J. Frechet, J. Phys. Chem. **97**, 293 (1993).

[22] P.M. Saville, P.A. Reynolds, J.W. White, C.J. Hawker, J.M.J. Frechet, K.L. Wooley, J. Penfold, and J.R.P. Webster, J. Phys. Chem. **99**, 8283 (1995).

[23] G.F. Kirton, A.S. Brown, C.J. Hawker, P.A. Reynolds, and J.W. White, Physica B **248**, 184 (1998).

[24] W.J. Pao, M.R. Stetzer, P.A. Heiney, W.D. Cho, and V. Percec, J. Phys. Chem. B **105**, 2170 (2001).

[25] C.A. Helm, L.A. Laxhuber, H. Möhwald, K. Kjaer, and J. Als-Nielsen, Biophys. J. **51**, A205 (1987).

[26] F. Gaboriaud, R. Golan, R. Volinsky, A. Berman, and R. Jelinek, Langmuir **17**, 3651 (2001).

[27] H.M. McConnell, Annu. Rev. Phys. Chem. **42**, 171 (1991).

[28] V. Percec, W.D. Cho, C. Mitchell, V.S.K. Balagurusamy, W.-J. Pao, P. Heiney, Y. Liu, and G. Ungar (unpublished).

[29] J. Als-Nielsen, D. Jacquemain, K. Kjaer, F. Leveiller, M. Lahav, and L. Leiserowitz, Phys. Rep. **246**, 252 (1994).

[30] K. Kjaer, J. Als-Nielsen, C.A. Helm, P. Tippmankrayer, and H. Möhwald, J. Phys. Chem. **93**, 3200 (1989).

[31] S.W. Barton, B.N. Thomas, E.B. Flom, S.A. Rice, B. Lin, J.B. Peng, J.B. Ketterson, and P. Dutta, J. Chem. Phys. **89**, 2257 (1988).

[32] T.M. Bohanon, B. Lin, M.C. Shih, G.E. Ice, and P. Dutta, Phys. Rev. B **41**, 4846 (1990).

[33] M.K. Durbin, A.G. Richter, C.-J. Yu, J.M. Kmetko, J.M. Bai, and P. Dutta, Phys. Rev. E **58**, 7686 (1998).

[34] *Phase Transitions in Soft Condensed Matter*, Vol. 211 of *NATO Advanced Study Institute, Series B: Physics*, edited by T. Riste and D.C. Sherrington (Plenum Press, New York, 1989).

[35] P. Tippmann-Krayer and H. Möhwald, Langmuir **7**, 2303 (1991).

[36] G. Ungar, J. Phys. Chem. **87**, 689 (1983).

[37] K. Larson, D. Vaknin, O. Villavicencio, D. McGrath, and V.V. Tsukruk, J. Phys. Chem. B **106**, 7246 (2002).

[38] K. Genson, D. Vaknin, O. Villavicencio, D. McGrath, and V. V. Tsukruk, J. Phys. Chem. B **106**, 11277 (2002).